Journal of Solid Mechanics Vol. 9, No. 3 (2017) pp. 490-507

Spectral Finite Element Method for Free Vibration of Axially Moving Plates Based on First-Order Shear Deformation Theory

M.R. Bahrami , S. Hatami *

Civil Engineering Department, Yasouj University, Yasouj, Iran

Received 30 May 2017; accepted 6 July 2017

ABSTRACT

In this paper, the free vibration analysis of moderately thick rectangular plates axially moving with constant velocity and subjected to uniform in-plane loads is investigated by the spectral finite element method. Two parallel edges of the plate are assumed to be simply supported and the remaining edges have any arbitrary boundary conditions. Using Hamilton's principle, three equations of motion for the plate are developed based on first-order shear deformation theory. The equations are transformed from the time domain into the frequency domain by assuming harmonic solutions. Then, the frequency-dependent dynamic shape functions obtained from the exact solution of the governing differential equations is used to develop the spectral stiffness matrix. By solving a non-standard eigenvalue problem, the natural frequencies and the critical speeds of the moving plates are obtained. The exactness and validity of the results are verified by comparing them with the results in previous studies. By the developed method some examples for vibration of stationary and moving moderately thick plates with different boundary conditions are presented. The effects of some parameters such as the axially speed of plate motion, the in-plane forces, aspect ratio and length to thickness ratio on the natural frequencies and the critical speeds of the moving plate are investigated. These results can be used as a benchmark for comparing the accuracy and precision of the other analytical and numerical methods.

Keywords: First-order shear deformation theory; Spectral finite element method; Transverse vibration; Axially moving; Dynamic stiffness matrix; Free vibration.

1 INTRODUCTION

AXIALLY moving plates are widely used in industry for variety applications. The bandsaw blades, the steel strip in a thin steel sheet production line, the belt and chain in power transmission, the high-speed magnetic or paper tape, the moving wide bands and belts, and the conveyor belts are some examples of axially moving plates. The axially speed may significantly affect the dynamic behavior of these structures. Therefore, investigating dynamic characteristics of moving plates is necessary for the analysis and design of these structures.

*Corresponding author. Tel.: +98 917 738 5476.
E-mail address: *hatami@yu.ac.ir* (Sh.Hatami).

In general, methods for solving dynamic problems of plates are divided into two categories, namely approximate or numerical methods and exact or analytical methods. The finite element method (FEM), finite strip method (FSM) and Rayleigh-Ritz method are some of the approximate methods. Ulsoy and Mote [1] developed transverse vibration analysis of wide bandsaw blades by Rayleigh-Ritz method. Lengoc and Mccallion [2] studied cutting conditions on the dynamic response of wide bandsaw blades using of Galerkin method. Based on Mindlin-Reissner plate theory, Wang [3] developed a FEM for a moving orthotropic thin plate. Luo and Hutton [4] presented formulation of the moving triangular plate element. The free vibration and stability analysis of axially moving viscoelastic thin plate were studied using of the differential quadrature method by Zhou and Wang [5]. Tang and Chen [6] investigated nonlinear free transverse vibration of the axially moving plates by multiple scales method. An and Su [7] obtained the dynamic response of axially moving orthotropic plates using the generalized integral transform technique. Eftekharia and Jafari [8] proposed dynamic analysis of the axially moving orthotropic rectangular plates subjected to linearly varying in-plane stress by high order accurate mixed finite element-differential quadrature method.

On the other hand, in the recent decade analytical methods have been used to extract the exact values for dynamic characteristics of the axially moving plates. The closed-form solution (CFS), exact finite strip method (EFSM) and dynamic stiffness method (DSM) are the exact analytical methods that considered by many researchers. Lin [9] investigated the stability and the vibration of axially moving plate subjected to uniform in-plane tension in transport direction using of the closed form solution. Equilibrium, membrane forces and buckling stability for thin plate axially traveling with high-speed are studied by Luo and Hamidzadeh [10]. The free vibration of the axially moving Levy-type viscoelastic thin plate was investigated by Marynowski [11]. Hatami et al. developed an exact finite strip method for axially moving isotropic plates [12], orthotropic plates on elastic foundation [13], laminated composite plates [14] and viscoelastic plates [15] subjected to in-plane forces, based on classical plate theory (CPT). By presenting a set of numerical examples, the effect of speed of plate motion and internal supports on the free vibration frequencies of the axially moving plates were studied [12-15]. The divergence velocities of axially moving orthotropic thin plates are investigated analytically via methods of complex analysis by Saksa and Jeronen [16].

Spectral Finite Element Method (SFEM) is a combination of dynamic stiffness method, spectral analysis method and finite element method. The SFEM provides dynamic responses in frequency domain due to the use of dynamic shape functions. The first step in SFEM is transforming the governing differential equations from time domain into frequency domain by assuming harmonic solutions. Then, the frequency-dependent dynamic shape functions obtained from the exact solution of the governing differential equations is used to develop the spectral stiffness matrix. The SFEM was developed for one-dimensional structures including the axially moving Bernouli-Euler beam by Oh et al. [17], the axially moving Timoshenko beam by Lee et al. [18] and the axially moving viscoelastic beam subjected to axial tension by Lee and Oh [19]. The SFEM also, was formulated for axially moving thin plates with constant speed subjected to uniform in-plane axial tension by Kim et al. [20] and axially moving beam-plates subjected to sudden external thermal loads by Kwon and Lee [21] based on CPT. According to the knowledge of the authors, the dynamic responses of moderately thick rectangular plates with axially moving speed using exact analytical methods have not been considered by any researcher, so far.

In the present paper, the free vibration analysis of moderately thick rectangular plates axially moving with constant velocity and subjected to uniform in-plane loads is investigated by the spectral finite element method. Two parallel edges of the plate are assumed to be simply supported and the remaining edges have any arbitrary boundary conditions (simply supported, clamped). The natural frequencies and critical speeds of axially moving plates are presented for three combinations of classical boundary conditions, namely CC, CS and SS. The mode shapes are presented for the transverse displacement of the plate. The effects of some parameters such as the in-plane forces, aspect ratio and length to thickness ratio on the natural frequencies and the critical speeds of the moving plate are investigated. The obtained dynamic responses are compared with available analytical or numerical solutions to confirm the validity and exactness of the results.

2 GOVERNING EQUATIONS OF AXIALLY MOVING FSDT PLATE

Consider a moderately thick rectangular plate moving with constant velocity c in the x-direction subjected to in-plane forces. The plate has the length L_x, width L_y and uniform thickness h, as shown in Fig. 1. The displacement fields of plate in x, y and z-direction are represented by $u(x,y,z,t)$, $v(x,y,z,t)$ and $w(x,y,z,t)$, respectively. Based on the first-order shear deformation theory (FSDT), the displacement fields for moderately thick rectangular plates, may be expressed as:

$$u(x,y,z,t)=z\,\phi_x(x,y,t) \quad , \quad v(x,y,z,t)=z\,\phi_y(x,y,t) \quad , \quad w(x,y,z,t)=w_0(x,y,t) \tag{1}$$

where ϕ_x and ϕ_y are the rotational displacements about the y and x axes at the middle surface of the plate, respectively, w_0 is the transverse displacement and t is the time variable. The strain-displacement relations for a moderately thick rectangular plate based on Eqs. (1) are defined as follows [22].

$$\varepsilon_{xx}=z\frac{\partial\phi_x}{\partial x} \quad , \quad \varepsilon_{yy}=z\frac{\partial\phi_y}{\partial y} \quad , \quad \varepsilon_{zz}=0 \quad , \quad \gamma_{xy}=z\left(\frac{\partial\phi_x}{\partial y}+\frac{\partial\phi_y}{\partial x}\right) \quad , \quad \gamma_{xz}=\frac{\partial w_0}{\partial x}+\phi_x \quad , \quad \gamma_{yz}=\frac{\partial w_0}{\partial y}+\phi_y \tag{2}$$

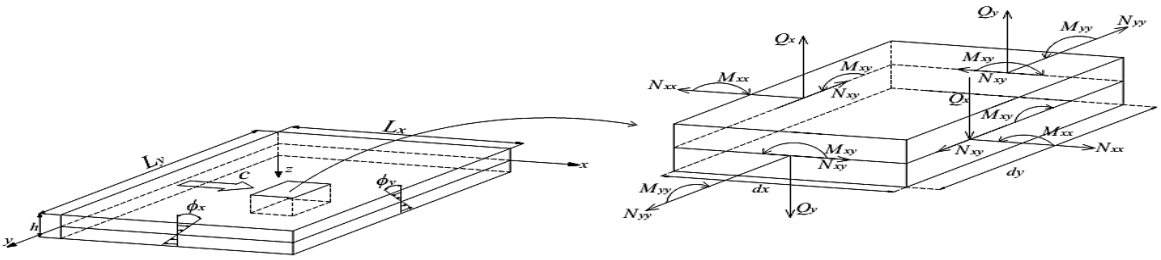

Fig.1
Displacement field, and internal forces and moments for an axially moving moderately thick plate.

The differential equations of motion and the boundary conditions of the plate are derived by Hamilton's principle, which is expressed in Eq. (3):

$$\begin{aligned}&\int_{t_1}^{t_2}(\delta U+\delta V-\delta K)dt=0\\&\delta w_0=\delta\phi_x=\delta\phi_y=0 \quad \text{at} \quad t=t_1,t_2\end{aligned} \tag{3}$$

where δU is the virtual strain energy and is defined as follows.

$$\delta U=\int_\Omega\left[\int_{-h/2}^{+h/2}\left(\sigma_{xx}\delta\varepsilon_{xx}+\sigma_{yy}\delta\varepsilon_{yy}+\sigma_{xy}\delta\gamma_{xy}+\sigma_{xz}\delta\gamma_{xz}+\sigma_{yz}\delta\gamma_{yz}\right)dz\right]dxdy \tag{4}$$

Substituting Eqs. (2) into Eq. (4), the virtual strain energy can be expressed as follows.

$$\delta U=\int_\Omega\left[M_{xx}\frac{\partial\delta\phi_x}{\partial x}+M_{yy}\frac{\partial\delta\phi_y}{\partial y}+M_{xy}\left(\frac{\partial\delta\phi_x}{\partial y}+\frac{\partial\delta\phi_y}{\partial x}\right)+Q_x\left(\frac{\partial\delta w_0}{\partial x}+\delta\phi_x\right)+Q_y\left(\frac{\partial\delta w_0}{\partial y}+\delta\phi_y\right)\right]dxdy \tag{5}$$

where the moments and transverse forces resulting from internal stress according to sign conventions shown in Fig. 1 are defined as follows.

$$\left[M_{xx}\quad M_{yy}\quad M_{xy}\right]=\int_{-h/2}^{+h/2}z\left[\sigma_{xx}\quad\sigma_{yy}\quad\sigma_{xy}\right]dz \ , \ \left[Q_x\quad Q_y\right]=k\int_{-h/2}^{+h/2}\left[\sigma_{xz}\quad\sigma_{yz}\right]dz \tag{6}$$

where k is the shear correction factor, which is obtained by Reissner as 5/6 [23]. We integrate by parts Eq. (5) to relieve the virtual generalized displacements ($\delta w_0,\delta\phi_x,\delta\phi_y$) in Ω of any differentiation. Then the virtual strain energy is given by:

$$\delta U = -\int_{\Omega}\left[\delta\phi_x\left(M_{xx,x}+M_{xy,y}-Q_x\right)+\delta\phi_y\left(M_{xy,x}+M_{yy,y}-Q_y\right)+\delta w_0\left(Q_{x,x}+Q_{y,y}\right)\right]dxdy$$
$$+\int_{\Gamma}\left[\delta\phi_x\left(M_{xx}n_x+M_{xy}n_y\right)+\delta\phi_y\left(M_{xy}n_x+M_{yy}n_y\right)+\delta w_0\left(Q_x n_x+Q_y n_y\right)\right]ds \tag{7}$$

where the comma followed by x or y parameter denotes differentiation with respect to the x or y, respectively. Also n_x and n_y are the components of the unit vector normal to the corresponding edge in x and y directions, respectively. The virtual work done by external forces δV_1 is given as follows:

$$\delta V_1 = -\int_{\Gamma}\left[\hat{Q}_x\delta w_0+\hat{M}_{xx}\delta\phi_x+\hat{M}_{xy}\delta\phi_y\right]\mathrm{d}y-\int_{\Gamma}\left[\hat{Q}_y\delta w_0+\hat{M}_{xy}\delta\phi_x+\hat{M}_{yy}\delta\phi_y\right]dx \tag{8}$$

where $\hat{Q}_x$,$\hat{Q}_y$,$\hat{M}_{xx}$,$\hat{M}_{yy}$ and $\hat{M}_{xy}$ are transverse shear forces and rotational moments per unit length imposed on the boundaries x=0, L_x and y=0, L_y. In the absence of N_{yy} and N_{xy}, the work done by the constant in-plane normal force N_{xx} (positive when tensile) acting in the x-direction is given as:

$$V_2 = \frac{1}{2}\int_{\Omega}N_{xx}\left(\frac{\partial w_0}{\partial x}\right)^2 dxdy \tag{9}$$

The virtual work due to Eq. (9) is rewritten as follows:

$$\delta V_2 = \int_{\Gamma}\bar{P}n_x\delta w_0 dy-\int_{\Omega}\bar{N}\delta w_0 dxdy \tag{10}$$

where

$$\bar{N} = N_{xx}\frac{\partial^2 w_0}{\partial x^2} \quad , \quad \bar{P} = N_{xx}\frac{\partial w_0}{\partial x} \tag{11}$$

The kinetic energy of the axially moving moderately thick plate is expressed as:

$$K = \frac{1}{2}\int_{\Omega}\left\{I_0\left[c^2+\left(\frac{\partial w_0}{\partial t}+c\frac{\partial w_0}{\partial x}\right)^2\right]+I_2\left[\left(\frac{\partial\phi_x}{\partial t}+c\frac{\partial\phi_x}{\partial x}\right)^2+\left(\frac{\partial\phi_y}{\partial t}\right)^2\right]\right\}\mathrm{d}x\mathrm{d}y \tag{12}$$

where $I_0 = \rho h$ and $I_2 = \rho h^3/12$ and ρ is the mass density of plate material. The virtual kinetic energy due to Eq. (12) is obtained as follows.

$$\delta K = \int_{\Omega}\left\{I_0\left[\left(\dot{w}_0+cw_0'\right)\times\left(\frac{\partial\delta w_0}{\partial t}+c\frac{\partial\delta w_0}{\partial x}\right)\right]+I_2\left[\left(\dot{\phi}_x+c\phi_x'\right)\times\left(\frac{\partial\delta\phi_x}{\partial t}+c\frac{\partial\delta\phi_x}{\partial x}\right)+\dot{\phi}_y\times\left(\frac{\partial\delta\phi_y}{\partial t}\right)\right]\right\}dxdy \tag{13}$$

In continuation, with respect to initial conditions and then integrating by parts to relieve the virtual generalized displacements ($\delta w_0, \delta\phi_x, \delta\phi_y$) in t of any differentiation

$$\int_{t_1}^{t_2}\delta K\,\mathrm{d}t = \int_{t_1}^{t_2}\left\{\begin{array}{l}-\int_{\Omega}\left[I_0\delta w_0\left(\ddot{w}_0+2c\dot{w}_0'+c^2w_0''\right)+I_2\delta\phi_x\left(\ddot{\phi}_x+2c\dot{\phi}_x'+c^2\phi_x''\right)+I_2\ddot{\phi}_y\delta\phi_y\right]\mathrm{d}x\mathrm{d}y\\ +\int_{\Gamma}\left[I_0\delta w_0\left(c\dot{w}_0+c^2w_0'\right)n_x+I_2\delta\phi_x\left(c\dot{\phi}_x+c^2\phi_x'\right)n_x\right]\mathrm{d}s\end{array}\right\}\mathrm{d}t \tag{14}$$

Finally, substituting the virtual strain energy δU, virtual work δV and virtual kinetic energy δK given by Eqs. (7), (8 and 10) and (14), respectively, into the Hamilton's principle in Eq. (3) and collecting the coefficients $\delta w_0, \delta\phi_x$ and $\delta\phi_y$, the governing differential equations of motion are obtained as:

$$\begin{aligned}
&\delta w_0: \quad Q_{x,x} + Q_{y,y} + \bar{N} = I_0(\ddot{w}_0 + 2c\dot{w}_0' + c^2 w_0'') \\
&\delta\phi_x: \quad M_{xx,x} + M_{xy,y} - Q_x = I_2(\ddot{\phi}_x + 2c\dot{\phi}_x' + c^2\phi_x'') \\
&\delta\phi_y: \quad M_{xy,x} + M_{yy,y} - Q_y = I_2\ddot{\phi}_y
\end{aligned} \tag{15}$$

and the natural boundary conditions on edges as:

$$\begin{aligned}
&\delta w_0: \quad Q_x n_x + Q_y n_y + \bar{P} - I_0(c\dot{w}_0 + c^2 w_0')n_x - \hat{Q}_x n_x - \hat{Q}_y n_y = 0 \\
&\delta\phi_x: \quad M_{xx} n_x + M_{xy} n_y - I_2(c\dot{\phi}_x + c^2\phi_x')n_x - \hat{M}_{xx} n_x - \hat{M}_{xy} n_y = 0 \\
&\delta\phi_y: \quad M_{xy} n_x + M_{yy} n_y - \hat{M}_{xy} n_x - \hat{M}_{yy} n_y = 0
\end{aligned} \tag{16}$$

Based on Hook's law, the relations between stress-strain are defined as follows [22]:

$$\sigma_{xx} = \frac{E}{1-\nu^2}\left(\varepsilon_{xx} + \nu\varepsilon_{yy}\right) \quad , \quad \sigma_{yy} = \frac{E}{1-\nu^2}\left(\varepsilon_{yy} + \nu\varepsilon_{xx}\right) \quad , \quad \sigma_{xy} = G\gamma_{xy} \quad , \quad \sigma_{xz} = G\gamma_{xz} \quad , \quad \sigma_{yz} = G\gamma_{yz} \tag{17}$$

where $G=E/2(1+\nu)$ is the shear modulus, E is the Young's modulus, and ν is the Poisson's ratio of the plate. Now, substituting Eqs. (2) and (17) into Eqs. (6), the resultant transverse shear forces Q_x, Q_y, bending moments M_{xx}, M_{yy}, and twisting moment M_{xy}, can be written with respect to the transverse displacement w_0, and rotational displacements about the y and x axes ϕ_x and ϕ_y, as follows.

$$\begin{Bmatrix} M_{xx} \\ M_{yy} \\ M_{xy} \end{Bmatrix} = D\begin{bmatrix} 1 & \nu & 0 \\ \nu & 1 & 0 \\ 0 & 0 & \dfrac{1-\nu}{2} \end{bmatrix}\begin{Bmatrix} \dfrac{\partial\phi_x}{\partial x} \\ \dfrac{\partial\phi_y}{\partial y} \\ \dfrac{\partial\phi_x}{\partial y} + \dfrac{\partial\phi_y}{\partial x} \end{Bmatrix} \quad , \quad \begin{Bmatrix} Q_x \\ Q_y \end{Bmatrix} = kGh\begin{bmatrix} 1 & 0 \\ 0 & 1 \end{bmatrix}\begin{Bmatrix} \dfrac{\partial w_0}{\partial x} + \phi_x \\ \dfrac{\partial w_0}{\partial y} + \phi_y \end{Bmatrix} \tag{18}$$

where $D=Eh^3/12(1-\nu^2)$ is the plate stiffness. Finally, substituting Eqs. (18) into Eqs. (15), the governing differential equations of motion in terms of displacements w_0, ϕ_x and ϕ_y can be expressed as:

$$\begin{aligned}
&kGh\left(\frac{\partial^2 w_0}{\partial x^2} + \frac{\partial\phi_x}{\partial x} + \frac{\partial^2 w_0}{\partial y^2} + \frac{\partial\phi_y}{\partial y}\right) + N_{xx}\frac{\partial^2 w_0}{\partial x^2} - \rho h\left(\frac{\partial^2 w_0}{\partial t^2} + 2c\frac{\partial^2 w_0}{\partial x\,\partial t} + c^2\frac{\partial^2 w_0}{\partial x^2}\right) = 0 \\
&D\left[\frac{\partial^2\phi_x}{\partial x^2} + \frac{1-\nu}{2}\frac{\partial^2\phi_x}{\partial y^2} + \frac{1+\nu}{2}\frac{\partial^2\phi_y}{\partial x\,\partial y}\right] - kGh\left(\frac{\partial w_0}{\partial x} + \phi_x\right) - \frac{\rho h^3}{12}\left(\frac{\partial^2\phi_x}{\partial t^2} + 2c\frac{\partial^2\phi_x}{\partial x\,\partial t} + c^2\frac{\partial^2\phi_x}{\partial x^2}\right) = 0 \\
&D\left[\frac{\partial^2\phi_y}{\partial y^2} + \frac{1-\nu}{2}\frac{\partial^2\phi_y}{\partial x^2} + \frac{1+\nu}{2}\frac{\partial^2\phi_x}{\partial x\,\partial y}\right] - kGh\left(\frac{\partial w_0}{\partial y} + \phi_y\right) - \frac{\rho h^3}{12}\frac{\partial^2\phi_y}{\partial t^2} = 0
\end{aligned} \tag{19}$$

3 SPECTRAL FINITE ELEMENT METHOD

3.1 Governing equations in the frequency domain

Fig. 2 shows a Levy-type plate in which two opposite edges (y=0 and L_y) are simply supported and the remaining

edges (x=0 and L_x) of the plate can have any arbitrary boundary conditions. The plate behavior in the y-direction, according to exact analytical solution method, can be represented in the form of a Fourier series. It should be noted that these functions must satisfy the boundary conditions along two parallel edges at y=0 and L_y. From now on, we only need to formulate a 1-D problem (along x axis) in SFEM. To obtain frequency-dependent dynamic shape function, it is necessary first to transform governing partial differential equations of motion from the time domain into the frequency domain by discrete Fourier transform (DFT). Then the spectral stiffness matrix using dynamic shape function by the force-displacement relation method is achieved. Based on Levy-type solution assumption and DFT theory, displacements w_0, ϕ_x and ϕ_y are represented in spectral form as follows.

$$\begin{aligned}
w_0(x,y,t) &= \frac{1}{N}\sum_{n=0}^{N-1}\sum_{m=1}^{\infty} W_{nm}(x,k_{ym},\omega_n)\sin(k_{ym}y)e^{i\omega_n t}\\
\phi_x(x,y,t) &= \frac{1}{N}\sum_{n=0}^{N-1}\sum_{m=1}^{\infty} \Phi_{xnm}(x,k_{ym},\omega_n)\sin(k_{ym}y)e^{i\omega_n t}\\
\phi_y(x,y,t) &= \frac{1}{N}\sum_{n=0}^{N-1}\sum_{m=1}^{\infty} \Phi_{ynm}(x,k_{ym},\omega_n)\cos(k_{ym}y)e^{i\omega_n t}
\end{aligned} \tag{20}$$

where $k_{ym}=m\pi/L_y$ and m is the number of half-wavelengths in direction y axis corresponding to terms of Fourier series and $i=\sqrt{-1}$ is the imaginary unit, N number of samples in the time domain and $\omega_n=2\pi n/T$ is nth discrete frequency, where T is sampling time window. W_{nm}, Φ_{ynm} and Φ_{xnm} are the spectral-modal components related to the displacements. By substituting Eqs. (20) into Eqs. (18), the resultant shear forces and moments can be rewritten in spectral forms as:

$$\begin{aligned}
M_{xx}(x,y,t) &= \frac{1}{N}\sum_{n=0}^{N-1}\sum_{m=1}^{\infty} M_{xxnm}(x,k_{ym},\omega_n)\sin(k_{ym}y)e^{i\omega_n t}\\
M_{yy}(x,y,t) &= \frac{1}{N}\sum_{n=0}^{N-1}\sum_{m=1}^{\infty} M_{yynm}(x,k_{ym},\omega_n)\sin(k_{ym}y)e^{i\omega_n t}\\
M_{xy}(x,y,t) &= \frac{1}{N}\sum_{n=0}^{N-1}\sum_{m=1}^{\infty} M_{xynm}(x,k_{ym},\omega_n)\cos(k_{ym}y)e^{i\omega_n t}
\end{aligned}
\qquad
\begin{aligned}
Q_x(x,y,t) &= \frac{1}{N}\sum_{n=0}^{N-1}\sum_{m=1}^{\infty} Q_{xnm}(x,k_{ym},\omega_n)\sin(k_{ym}y)e^{i\omega_n t}\\
Q_y(x,y,t) &= \frac{1}{N}\sum_{n=0}^{N-1}\sum_{m=1}^{\infty} Q_{xnm}(x,k_{ym},\omega_n)\cos(k_{ym}y)e^{i\omega_n t}
\end{aligned} \tag{21}$$

where M_{xxnm}, M_{yynm}, M_{xynm}, Q_{xnm} and Q_{ynm} are the spectral-modal components given by:

$$\begin{aligned}
M_{xxnm}(x,k_{ym},\omega_n) &= D\left(\frac{\mathrm{d}\Phi_{xnm}}{\mathrm{d}x} - k_{ym}\nu\Phi_{ynm}\right)\\
M_{yynm}(x,k_{ym},\omega_n) &= D\left(-k_{ym}\Phi_{ynm} + \nu\frac{\mathrm{d}\Phi_{xnm}}{\mathrm{d}x}\right)\\
M_{xynm}(x,k_{ym},\omega_n) &= \frac{Gh^3}{12}\left(k_{ym}\Phi_{xnm} + \frac{\mathrm{d}\Phi_{ynm}}{\mathrm{d}x}\right)
\end{aligned}
\qquad
\begin{aligned}
Q_{xnm}(x,k_{ym},\omega_n) &= kGh\left(\frac{\mathrm{d}W_{nm}}{\mathrm{d}x} + \Phi_{xnm}\right)\\
Q_{ynm}(x,k_{ym},\omega_n) &= kGh\left(k_{ym}W_{nm} + \Phi_{ynm}\right)
\end{aligned} \tag{22}$$

Substituting Eqs. (20) into Eqs. (19) yields a set of coupled ordinary differential equations in the frequency domain as:

$$\begin{aligned}
&\left(kGh + N_{xx} - \rho hc^2\right)\frac{\mathrm{d}^2W_{nm}}{\mathrm{d}x^2} - 2c\rho hi\,\omega_n\frac{\mathrm{d}W_{nm}}{\mathrm{d}x} + \left(\rho h\omega_n^2 - kGhk_{ym}^2\right)W_{nm} + kGh\frac{\mathrm{d}\Phi_{xnm}}{\mathrm{d}x} - kGhk_{ym}\Phi_{ynm} = 0\\
&\left(D - \frac{\rho h^3c^2}{12}\right)\frac{\mathrm{d}^2\Phi_{xnm}}{\mathrm{d}x^2} - \frac{c\rho h^3 i\,\omega_n}{6}\frac{\mathrm{d}\Phi_{xnm}}{\mathrm{d}x} + \left(\frac{\rho h^3\omega_n^2}{12} - Dk_{ym}^2\frac{1-\nu}{2} - kGh\right)\Phi_{xnm} - Dk_{ym}\frac{1+\nu}{2}\frac{\mathrm{d}\Phi_{ynm}}{\mathrm{d}x} - kGh\frac{\mathrm{d}W_{nm}}{\mathrm{d}x} = 0\\
&\left(D\frac{1-\nu}{2}\right)\frac{\mathrm{d}^2\Phi_{ynm}}{\mathrm{d}x^2} + \left(\frac{\rho h^3\omega_n^2}{12} - Dk_{ym}^2 - kGh\right)\Phi_{ynm} + Dk_{ym}\frac{1+\nu}{2}\frac{\mathrm{d}\Phi_{xnm}}{\mathrm{d}x} - kGh\,k_{ym}W_{nm} = 0
\end{aligned} \tag{23}$$

Since n_y=0 on edges x=0 and x=L_x, by substituting Eqs. (20) and (21) into Eqs. (16), the boundary values on these edges can be rewritten in spectral forms as:

$$\begin{aligned}
\hat{Q}_x(x,y,t) &= \frac{1}{N}\sum_{n=0}^{N-1}\sum_{m=1}^{\infty}\hat{Q}_{xnm}(x,k_{ym},\omega_n)\sin(k_{ym}y)e^{i\omega_n t} \\
\hat{M}_{xx}(x,y,t) &= \frac{1}{N}\sum_{n=0}^{N-1}\sum_{m=1}^{\infty}\hat{M}_{xxnm}(x,k_{ym},\omega_n)\sin(k_{ym}y)e^{i\omega_n t} \\
\hat{M}_{xy}(x,y,t) &= \frac{1}{N}\sum_{n=0}^{N-1}\sum_{m=1}^{\infty}\hat{M}_{xynm}(x,k_{ym},\omega_n)\cos(k_{ym}y)e^{i\omega_n t}
\end{aligned} \tag{24}$$

where $\hat{Q}_{xnm}$, $\hat{M}_{xxnm}$ and $\hat{M}_{xynm}$ are the spectral components and the force-displacement relationships in the frequency domain can be expressed as follows.

$$\begin{aligned}
\hat{Q}_{xnm} &= Q_{xnm} + N_{xx}\frac{\mathrm{d}W_{nm}}{\mathrm{d}x} - \rho h\,(ci\,\omega_n W_{nm} + c^2\frac{\mathrm{d}W_{nm}}{\mathrm{d}x}) \\
\hat{M}_{xxnm} &= M_{xxnm} - \frac{\rho h^3}{12}(ci\,\omega_n \Phi_{xnm} + c^2\frac{\mathrm{d}\Phi_{xnm}}{\mathrm{d}x}) \\
\hat{M}_{xynm} &= M_{xynm}
\end{aligned} \tag{25}$$

3.2 Spectral element equation

3.2.1 General solution of spectral-modal displacements

The dynamic (frequency-dependent) shape functions are obtained from general solution of the governing differential equations. Assume the general solutions of Eqs. (23) is as follows.

$$W_{nm} = \alpha b_{nm} e^{k_{xnm}x} \quad , \quad \Phi_{xnm} = b_{nm} e^{k_{xnm}x} \quad , \quad \Phi_{ynm} = \beta b_{nm} e^{k_{xnm}x} \tag{26}$$

where k_{xnm} are wavenumbers in direction x axis and b_{nm} the constant coefficient. Substituting Eqs. (26) into Eqs. (23) an eigenvalue problem is obtained.

$$\begin{bmatrix} T_{11} & T_{12} & T_{13} \\ T_{21} & T_{22} & T_{23} \\ T_{31} & T_{32} & T_{33} \end{bmatrix} \begin{Bmatrix} \alpha \\ 1 \\ \beta \end{Bmatrix} b_{nm} = \begin{Bmatrix} 0 \\ 0 \\ 0 \end{Bmatrix} \tag{27}$$

where

$$\begin{aligned}
&T_{11} = \left(kGh + N_{xx} - \rho hc^2\right)k_{xnm}^2 - 2c\,\rho hi\,\omega_n k_{xnm} + \rho h\omega_n^2 - kGhk_{ym}^2 \quad , \quad T_{12} = kGhk_{xnm} \quad , \quad T_{13} = -kGhk_{ym} \\
&T_{21} = -kGh\,k_{xnm} \quad , \quad T_{22} = \left(D - \frac{\rho h^3 c^2}{12}\right)k_{xnm}^2 - \frac{c\,\rho h^3 i\,\omega_n}{6}k_{xnm} + \frac{\rho h^3\omega_n^2}{12} - Dk_{ym}^2\frac{1-\nu}{2} - kGh \quad , \quad T_{23} = -Dk_{ym}\frac{1+\nu}{2}k_{xnm} \\
&T_{31} = -kGh\,k_{ym} \quad , \quad T_{32} = Dk_{ym}\frac{1+\nu}{2}k_{xnm} \quad , \quad T_{33} = \left(D\frac{1-\nu}{2}\right)k_{xnm}^2 + \frac{\rho h^3\omega_n^2}{12} - Dk_{ym}^2 - kGh
\end{aligned} \tag{28}$$

The algebraic Eq. (27) has a nontrivial solution, which is obtained by setting determinant of the coefficients matrix as zero. Hence, after simplification, it yields a six order polynomial in terms of wavenumbers.

$$m_1 k_{xnm}^6 + m_2 k_{xnm}^5 + m_3 k_{xnm}^4 + m_4 k_{xnm}^3 + m_5 k_{xnm}^2 + m_6 k_{xnm} + m_7 = 0 \tag{29}$$

where

$$m_1=\frac{1}{24}D(\nu-1)\left(Ghk+N_{xx}-\rho hc^2\right)\left(\rho h^3c^2-12D\right)$$

$$m_2=\frac{1}{12}\rho hDci\,\omega_n(\nu-1)\left[12D+h^2\left(Ghk+N_{xx}-2\rho hc^2\right)\right]$$

$$m_3=\frac{1}{144}\begin{Bmatrix}72D^2(\nu-1)\left[3Ghkk_{ym}^2+2k_{ym}^2\left(N_{xx}-\rho hc^2\right)-\rho h\omega_n^2\right]+\rho h^4c^2\left(12Gk-\rho h^2\omega_n^2\right)\left(Ghk+N_{xx}-\rho hc^2\right)\\ -6Dh\begin{bmatrix}24G^2hk^2-Gk(\nu-3)\left(12N_{xx}-\rho h\left\langle 12c^2+c^2h^2k_{ym}^2+h^2\omega_n^2\right\rangle\right)\\ +\rho h^2\left(2c^4\rho hk_{ym}^2+N_{xx}\omega_n^2(\nu-3)-2c^2\left\langle N_{xx}k_{ym}^2-4\rho h\omega_n^2+3\rho h\nu\omega_n^2\right\rangle\right)\end{bmatrix}\end{Bmatrix}$$

$$m_4=-\frac{1}{72}\rho hci\,\omega_n\begin{Bmatrix}144D^2k_{ym}^2(\nu-1)+h^3\left(Ghk+N_{xx}-2\rho hc^2\right)\left(\rho h^2\omega_n^2-12Gk\right)\\ +6Dh\left[Gk\left(12+h^2k_{ym}^2\right)(\nu-3)+2h\left(-k_{ym}^2\left\langle N_{xx}-2\rho hc^2\right\rangle-2\rho h\omega_n^2(\nu-2)\right)\right]\end{Bmatrix}$$

$$m_5=\frac{1}{144}\begin{Bmatrix}72D^2k_{ym}^2(1-\nu)\left[3Ghkk_{ym}^2+k_{ym}^2\left(N_{xx}-\rho hc^2\right)-2\rho h\omega_n^2\right]+\\ h^2\begin{bmatrix}\rho^2h^4\omega_n^4\left(N_{xx}-6\rho hc^2\right)+12G^2k^2\left(12N_{xx}-\rho h\left\langle 12c^2+h^2\omega_n^2\right\rangle\right)+\\ Gk\,\rho h^2\omega_n^2\left(-24N_{xx}+\rho h\left\langle 84c^2+c^2h^2k_{ym}^2+h^2\omega_n^2\right\rangle\right)\end{bmatrix}+\\ 6Dh\begin{bmatrix}48G^2hk^2k_{ym}^2+\rho h^2\omega_n^2\left(N_{xx}k_{ym}^2(\nu-3)-\rho hc^2k_{ym}^2(\nu-13)-\rho h\omega_n^2(\nu-3)\right)-\\ 2Gk\left(\rho h^3c^2k_{ym}^4-6\rho h\omega_n^2(\nu-3)+k_{ym}^2(\nu-3)\left\langle 6N_{xx}-6\rho hc^2-\rho h^3\omega_n^2\right\rangle\right)\end{bmatrix}\end{Bmatrix} \tag{30}$$

$$m_6=\frac{1}{72}\rho hci\,\omega_n\begin{Bmatrix}-144G^2h^2k^2+\left(24Dk_{ym}^2-2\rho h^3\omega_n^2\right)\left(3Dk_{ym}^2(\nu-1)+\rho h^3\omega_n^2\right)\\ +Ghk\left[-12Dk_{ym}^2\left(18+h^2k_{ym}^2-6\nu\right)+\rho h^3\omega_n^2\left(36+h^2k_{ym}^2\right)\right]\end{Bmatrix}$$

$$m_7=-\frac{1}{144}h\left(-12Ghk+6Dk_{ym}^2(\nu-1)+\rho h^3\omega_n^2\right)\left\{\rho h\omega_n^2\left[Gk\left(12+h^2k_{ym}^2\right)-\rho h^2\omega_n^2\right]-12D\left(Gkk_{ym}^4-\rho\omega_n^2k_{ym}^2\right)\right\}$$

Eq. (29) is known as the dispersion relation or spectrum relation. There is no general formula for computing the latent roots of a polynomial of degree five or greater. Thus, from a practical point view, the approximate latent roots that are accurate enough for the desired precision will be as useful as the exact ones [24]. The coefficients α and β corresponding to each wavenumber obtained from Eqs. (27) are as follows.

$$\alpha=-\frac{T_{12}T_{23}-T_{13}T_{22}}{T_{11}T_{23}-T_{13}T_{21}}\quad,\quad\beta=-\frac{T_{12}T_{21}-T_{11}T_{22}}{T_{13}T_{21}-T_{11}T_{23}} \tag{31}$$

or

$$\alpha_i=-\frac{Ghk\left[\rho h^3c^2k_{xnmi}^2+2\rho h^3ci\,\omega_nk_{xnmi}+6Dk_{xnmi}^2(\nu-1)+6Dk_{ym}^2(1-\nu)+12Ghk-\rho h^3\omega_n^2\right]}{6k_{xnmi}\left[2G^2h^2k^2+(\nu+1)\begin{pmatrix}-D\rho hc^2k_{xnmi}^2-2D\rho hci\,\omega_nk_{xnmi}+DGhkk_{xnmi}^2\\ -DGhkk_{ym}^2+D\rho h\omega_n^2+DN_{xx}k_{xnmi}^2\end{pmatrix}\right]}$$

$$\beta_i=-\frac{\begin{bmatrix}-G^2h^2k^2k_{xnmi}^2-\left(k_{xnmi}^2\left\langle Ghk+N_{xx}-\rho hc^2\right\rangle-2\rho hci\,\omega_nk_{xnmi}-Ghkk_{ym}^2+\rho h\omega_n^2\right)\\ \left(k_{xnmi}^2\left\langle D-\frac{1}{12}\rho h^3c^2\right\rangle-\frac{1}{6}\rho h^3ci\,\omega_nk_{xnmi}-\frac{1}{2}Dk_{ym}^2(1-\nu)-Ghk+\frac{1}{12}\rho h^3\omega_n^2\right)\end{bmatrix}}{\left[G^2h^2k^2k_{ym}k_{xnmi}+\frac{1}{2}Dk_{ym}k_{xnmi}(1+\nu)\left(k_{xnmi}^2\left\langle Ghk+N_{xx}-\rho hc^2\right\rangle-2\rho hci\,\omega_nk_{xnmi}-Ghkk_{ym}^2+\rho h\omega_n^2\right)\right]} \tag{32}$$

Finally, the general solutions of Eqs. (23) is presented as follows.

$$W_{nm} = E_{nm}^{\mathrm{T}}(x, k_{ym}, \omega_n)\alpha_p b_{nm} \quad , \quad \Phi_{xnm} = E_{nm}^{\mathrm{T}}(x, k_{ym}, \omega_n) b_{nm} \quad , \quad \Phi_{ynm} = E_{nm}^{\mathrm{T}}(x, k_{ym}, \omega_n)\beta_p b_{nm} \tag{33}$$

where

$$\begin{aligned} E_{nm}^{\mathrm{T}}(x, k_{ym}, \omega_n) &= \begin{bmatrix} e^{k_{xnm1}x} & e^{k_{xnm2}x} & e^{k_{xnm3}x} & e^{k_{xnm4}x} & e^{k_{xnm5}x} & e^{k_{xnm6}x} \end{bmatrix} \\ b_{nm} &= \begin{bmatrix} b_{nm1} & b_{nm2} & b_{nm3} & b_{nm4} & b_{nm5} & b_{nm6} \end{bmatrix}^{\mathrm{T}} \end{aligned} \tag{34}$$

and

$$\alpha_p = \mathrm{diag}[\alpha_i] = \mathrm{diag}\begin{bmatrix} \alpha_1 & \alpha_2 & \alpha_3 & \dots & \alpha_6 \end{bmatrix}_{6\times 6} \quad , \quad \beta_p = \mathrm{diag}[\beta_i] = \mathrm{diag}\begin{bmatrix} \beta_1 & \beta_2 & \beta_3 & \dots & \beta_6 \end{bmatrix}_{6\times 6} \tag{35}$$

3.2.2 Spectral-modal nodal DOFs vector

For a spectral finite element shown in Fig. 2(b), the geometric boundary conditions must be satisfied at the element nodes ($x = x_1$ and $x = x_2$). The geometric boundary conditions include the transverse displacement and rotational displacements about the y and x axes. The spectral-modal nodal degrees of freedom (DOFs) for the axially moving moderately thick rectangular plate element are specified in Fig. 2(b). The spectral-modal nodal DOFs vector d_{nm} can be defined by applying the geometric boundary conditions, as follows.

$$\begin{aligned} d_{nm} &= \begin{Bmatrix} W_{nm1} & \Phi_{xnm1} & \Phi_{ynm1} & W_{nm2} & \Phi_{xnm2} & \Phi_{ynm2} \end{Bmatrix}^{\mathrm{T}} \\ &= \begin{Bmatrix} W_{nm}(x_1) & -\Phi_{xnm}(x_1) & \Phi_{ynm}(x_1) & W_{nm}(x_2) & -\Phi_{xnm}(x_2) & \Phi_{ynm}(x_2) \end{Bmatrix}^{\mathrm{T}} \end{aligned} \tag{36}$$

Substituting Eqs. (33) into Eq. (36) yields the relationship as:

$$d_{nm} = G_{nm}(k_{ym}, \omega_n) b_{nm} \tag{37}$$

where

$$G_{nm}(k_{ym}, \omega_n) = \begin{bmatrix} \alpha_1 e^{k_{xnm1}x_1} & \alpha_2 e^{k_{xnm2}x_1} & \dots & \alpha_6 e^{k_{xnm6}x_1} \\ -e^{k_{xnm1}x_1} & -e^{k_{xnm2}x_1} & \dots & -e^{k_{xnm6}x_1} \\ \beta_1 e^{k_{xnm1}x_1} & \beta_2 e^{k_{xnm2}x_1} & \dots & \beta_6 e^{k_{xnm6}x_1} \\ \alpha_1 e^{k_{xnm1}x_2} & \alpha_2 e^{k_{xnm2}x_2} & \dots & \alpha_6 e^{k_{xnm6}x_2} \\ -e^{k_{xnm1}x_2} & -e^{k_{xnm2}x_2} & \dots & -e^{k_{xnm6}x_2} \\ \beta_1 e^{k_{xnm1}x_2} & \beta_2 e^{k_{xnm2}x_2} & \dots & \beta_6 e^{k_{xnm6}x_2} \end{bmatrix}_{6\times 6} \tag{38}$$

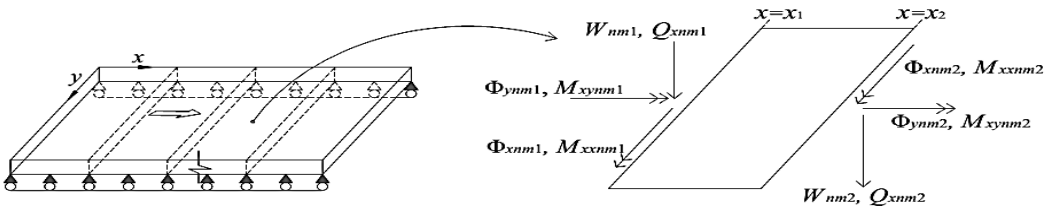

(a) dividing the plate to some elements (b) spectral finite element

Fig.2
Sign conventions spectral-modal nodal DOFs and forces.

3.2.3 Dynamic shape functions

By eliminating the constant vector b_{nm} from Eqs. (33) by using Eq. (37), the general solutions of the governing ordinary differential equations of motion in the frequency domain (relations Eqs. (23)) in terms of the spectral-modal nodal DOFs vector d_{nm} are expressed as follows.

$$W_{nm} = N_{Wnm}^{\mathrm{T}} d_{nm} \quad , \quad \Phi_{xnm} = N_{\Phi xnm}^{\mathrm{T}} d_{nm} \quad , \quad \Phi_{ynm} = N_{\Phi ynm}^{\mathrm{T}} d_{nm} \tag{39}$$

where $N_{Wnm}^{\mathrm{T}}, N_{\Phi xnm}^{\mathrm{T}}$ and $N_{\Phi ynm}^{\mathrm{T}}$ are the dynamic (frequency-dependent) shape functions related to spectral-modal displacements W_{nm}, Φ_{xnm} and Φ_{ynm}, respectively. They are obtained from the exact solution of the governing differential equations and are defined as follows. The dynamic shape functions are 1-by-6 matrices.

$$N_{Wnm}^{\mathrm{T}}(x, k_{ym}, \omega_n) = E_{nm}^{\mathrm{T}} \alpha_p G_{nm}^{-1} \ , \quad N_{\Phi xnm}^{\mathrm{T}}(x, k_{ym}, \omega_n) = E_{nm}^{\mathrm{T}} G_{nm}^{-1} \ , \quad N_{\Phi ynm}^{\mathrm{T}}(x, k_{ym}, \omega_n) = E_{nm}^{\mathrm{T}} \beta_p G_{nm}^{-1} \tag{40}$$

3.2.4 Spectral-modal nodal forces vector

Substituting Eqs. (33) into Eqs. (22) and (25), the force-displacement relationships in the frequency domain can be rewritten as follows.

$$\begin{aligned}
\hat{Q}_{xnm}(x, k_{ym}, \omega_n) &= \sum_{i=1}^{6} b_{nmi} \left[kGh\left(\alpha_i k_{xnmi} + 1\right) + N_{xx}\left(\alpha_i k_{xnmi}\right) - \rho h\left(ci\,\omega_n \alpha_i + c^2 \alpha_i k_{xnmi}\right) \right] e^{k_{xnmi} x} \\
\hat{M}_{xxnm}(x, k_{ym}, \omega_n) &= \sum_{i=1}^{6} b_{nmi} \left[D\left(k_{xnmi} - k_{ym} \nu \beta_i\right) - \frac{\rho h^3}{12}\left(ci\,\omega_n + c^2 k_{xnmi}\right) \right] e^{k_{xnmi} x} \\
\hat{M}_{xynm}(x, k_{ym}, \omega_n) &= \sum_{i=1}^{6} b_{nmi} \left[\frac{Gh^3}{12}\left(k_{ym} + \beta_i k_{xnmi}\right) \right] e^{k_{xnmi} x}
\end{aligned} \tag{41}$$

For a spectral finite element shown in Fig. 2(b), the natural boundary conditions at the element nodes ($x = x_1$ and $x = x_2$) must be satisfied. The natural boundary conditions in the frequency domain include the spectral-modal transverse shear force $\hat{Q}_{xnm}$, spectral-modal bending moment $\hat{M}_{xxnm}$ and spectral-modal twisting moment $\hat{M}_{xynm}$. The spectral-modal nodal force and moments for the moderately thick rectangular plate element are shown in Fig. 2(b). The spectral-modal nodal forces vector f_{nm} can be obtained by applying the natural boundary conditions, and given the sign conventions used in the theory of the plate (shown in Fig. 1), they are written as follows.

$$\begin{aligned}
f_{nm} &= \left\{ \hat{Q}_{xnm1} \quad \hat{M}_{xxnm1} \quad \hat{M}_{xynm1} \quad \hat{Q}_{xnm2} \quad \hat{M}_{xxnm2} \quad \hat{M}_{xynm2} \right\}^{\mathrm{T}} \\
&= \left\{ -\hat{Q}_{xnm}(x_1) \quad -\hat{M}_{xxnm}(x_1) \quad \hat{M}_{xynm}(x_1) \quad \hat{Q}_{xnm}(x_2) \quad \hat{M}_{xxnm}(x_2) \quad -\hat{M}_{xynm}(x_2) \right\}^{\mathrm{T}}
\end{aligned} \tag{42}$$

Substituting Eqs. (41) into Eq. (42) yields the relationship as:

$$f_{nm} = R_{nm}(k_{ym}, \omega_n) b_{nm} \tag{43}$$

where

$$R_{nm}(k_{ym}, \omega_n) = \begin{bmatrix}
-A_1 e^{k_{xnm1} x_1} & -A_2 e^{k_{xnm2} x_1} & \dots & -A_6 e^{k_{xnm6} x_1} \\
-B_1 e^{k_{xnm1} x_1} & -B_2 e^{k_{xnm2} x_1} & \dots & -B_6 e^{k_{xnm6} x_1} \\
-C_1 e^{k_{xnm1} x_1} & -C_2 e^{k_{xnm2} x_1} & \dots & -C_6 e^{k_{xnm6} x_1} \\
A_1 e^{k_{xnm1} x_2} & A_2 e^{k_{xnm2} x_2} & \dots & A_6 e^{k_{xnm6} x_2} \\
B_1 e^{k_{xnm1} x_2} & B_2 e^{k_{xnm2} x_2} & \dots & B_6 e^{k_{xnm6} x_2} \\
C_1 e^{k_{xnm1} x_2} & C_2 e^{k_{xnm2} x_2} & \dots & C_6 e^{k_{xnm6} x_2}
\end{bmatrix}_{6\times 6} \tag{44}$$

and

$$\begin{aligned} A_i &= kGh\ (\alpha_i k_{xnmi} + 1) + N_{xx}\alpha_i k_{xnmi} - \rho h(ci\,\omega_n \alpha_i + c^2 \alpha_i k_{xnmi}) \\ B_i &= D(k_{xnmi} - k_{ym}\nu\beta_i) - \frac{\rho h^3}{12}(ci\,\omega_n + c^2 k_{xnmi}) \qquad , \quad (i = 1, 2, \ldots, 6) \\ C_i &= -\frac{Gh^3}{12}(k_{ym} + \beta_i k_{xnmi}) \end{aligned} \tag{45}$$

3.2.5 Spectral stiffness matrix

Eliminating the constant coefficients vector b_{nm} from Eq. (43) using Eq. (37) gives the relationship between the spectral-modal nodal forces vector f_{nm} and the spectral-modal nodal DOFs vector d_{nm} as follows. This relationship is known in the literature as spectral element equation.

$$f_{nm} = S_{nm} d_{nm} \tag{46}$$

where

$$S_{nm}(k_{ym}, \omega_n) = R_{nm} G_{nm}^{-1} \tag{47}$$

The matrix S_{nm} is known as exact dynamic (frequency-dependent) stiffness matrix. In the literature it is often called spectral element matrix or spectral stiffness matrix. Also the matrix S_{nm} is a six-by-six and symmetric matrix. The present spectral stiffness matrix is formulated for the axially moving moderately thick rectangular plate element based on FSDT.

4 FREE VIBRATION ANALYSIS

To analyze the vibration of a plate by SFEM it is required to divide plate into some elements as shown in Fig. 2(a). Following that, the spectral-modal nodal DOFs and forces at each node of the spectral finite elements could be defined. The spectral element equation explained in Eq. (46) can be assembled by using a method similar to that used in the conventional finite element method. Finally, global system equation is given as follows.

$$f_{gnm} = S_{gnm}(k_{ym}, \omega_n) d_{gnm} \tag{48}$$

where S_{gnm} is the global spectral stiffness matrix, d_{gnm} is the global spectral-modal nodal DOFs vector and f_{gnm} is the global spectral-modal nodal forces vector. The boundary conditions along the edges parallel to the y axis for simply supported and clamped cases can be expressed by Eqs. (49) and (50), respectively.

Simply Supported (S)

$$\begin{aligned} &W_{nm}(x, k_{ym}, \omega_n) = 0 \quad , \quad M_{xxnm}(x, k_{ym}, \omega_n) = 0 \quad , \quad \Phi_{xnm}(x, k_{ym}, \omega_n) = 0 \\ &Q_{xnm}(x, k_{ym}, \omega_n) \neq 0 \quad , \quad \Phi_{ynm}(x, k_{ym}, \omega_n) \neq 0 \quad , \quad M_{xynm}(x, k_{ym}, \omega_n) \neq 0 \end{aligned} \tag{49}$$

Clamped (C)

$$\begin{aligned} &W_{nm}(x, k_{ym}, \omega_n) = 0 \quad , \quad \Phi_{ynm}(x, k_{ym}, \omega_n) = 0 \quad , \quad \Phi_{xnm}(x, k_{ym}, \omega_n) = 0 \\ &Q_{xnm}(x, k_{ym}, \omega_n) \neq 0 \quad , \quad M_{xxnm}(x, k_{ym}, \omega_n) \neq 0 \quad , \quad M_{xynm}(x, k_{ym}, \omega_n) \neq 0 \end{aligned} \tag{50}$$

Fig. 3 shows three different combinations of boundary conditions expressed in Eqs. (49) and (50), namely CC, CS, and SS. The boundary conditions of two parallel edges at y=0 and L_y that are simply supported are not written for brevity.

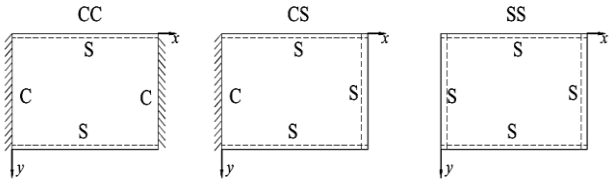

Fig.3
Three combinations of boundary conditions for axially moving moderately thick rectangular plate.

After applying the associated boundary conditions on the assembled set of equations, the final form of the global system equation is obtained.

$$\bar{f}_{gnm} = \bar{S}_{gnm}(k_{ym}, \omega_n)\bar{d}_{gnm} \tag{51}$$

By setting $\bar{f}_{gnm}$ to zero, the eigenvalue problem for free vibration of the intended plate can be obtained.

$$\bar{S}_{gnm}(k_{ym}, \omega_n)\bar{d}_{gnm} = 0 \tag{52}$$

By setting the determinant of $\bar{S}_{gnm}$ to zero, the natural frequencies, ω_{NAT}, are determined.

$$\det\left(\bar{S}_{gnm}(k_{ym}, \omega_n)\right) = 0 \tag{53}$$

Eq. (52) is a transcendental eigenvalue problem. Therefore, the traditional procedures for solving the linear eigenvalue problem are not applicable. In earlier publications, various methods including Wittrick-Williams algorithm and method of trial and error to obtain the natural frequencies of Eq. (53) were suggested. In the present paper an efficient numerical algorithm using drawing method described in Ref. [14] is used. In this procedure, the variation of stiffness matrix determinant $\det(\bar{S}_{gnm})$ in logarithmic scale versus discrete frequencies ω_n is plotted for different values of half-wavelengths, m. The points on the horizontal axis in which the logarithmic function tends to negative infinity are natural frequencies. Substituting these natural frequencies into Eq. (52), corresponding mode shapes can be computed.

5 NUMERICAL RESULTS AND DISCUSSION

For programing the formulations of the present SFEM and extracting the free vibration frequencies, critical speeds and mode shapes mathematica software is used. Different in-plane normal forces, boundary conditions, aspect ratios, length to thickness ratio of plate and also different axial speed are considered in the results presented in this article. The dimensionless variables used in the results are introduced as:

$$\bar{\omega} = \omega_n \frac{L_y^2}{2\pi^2}\sqrt{\rho h / D} \quad , \quad \psi = c\frac{L_y}{\pi}\sqrt{\rho h / D} \quad , \quad k_x = \frac{N_x L_y^2}{\pi^2 D} \tag{54}$$

where $\bar{\omega}$ and ψ are dimensionless natural frequency and, traveling speed respectively, and k_x is in-plane load parameter along x-direction. The parameter m in the results implies the number of half-wavelengths along the y-direction and the parameter n is the root number in the characteristic function of Eq. (53). It should be mentioned that there is an infinite number of roots for this function.

5.1 Validity

The accuracy and excellent performance of the SFEM against the results available in the literature are investigated. At first, exact frequencies of free transverse vibration of Levy-type rectangular plates without axially speed (c=0)

are calculated based on FSDT with various boundary conditions. For this purpose, an isotropic square plate (L_x=L_y) with length to thickness ratio of 10 (L_x/h=10) is considered and the shear correction factor and Poisson's ratio are assumed as 5/6 and 0.3, respectively. Also, plate not subjected any in-plane forces (N_{xx}=0). Fig. 4 shows the variation of Log (Abs (Det[$\bar{S}_{gnm}(k_{ym},\omega_n)$])) with respect to frequency parameter $\bar{\omega}$ for different values of half-wavelengths along y-direction, m. As mentioned in Sec. 4, the points on the horizontal axis in which the logarithmic function tends to negative infinity are natural frequencies. As shown in the Fig. 4(a), for the case boundary condition, CC of the first and the third frequency parameter corresponds to the first mode in direction y axis (m=1), the second and the fourth frequency parameter is associated with second mode (m=2) and fifth frequency parameter of the third mode (m=3).

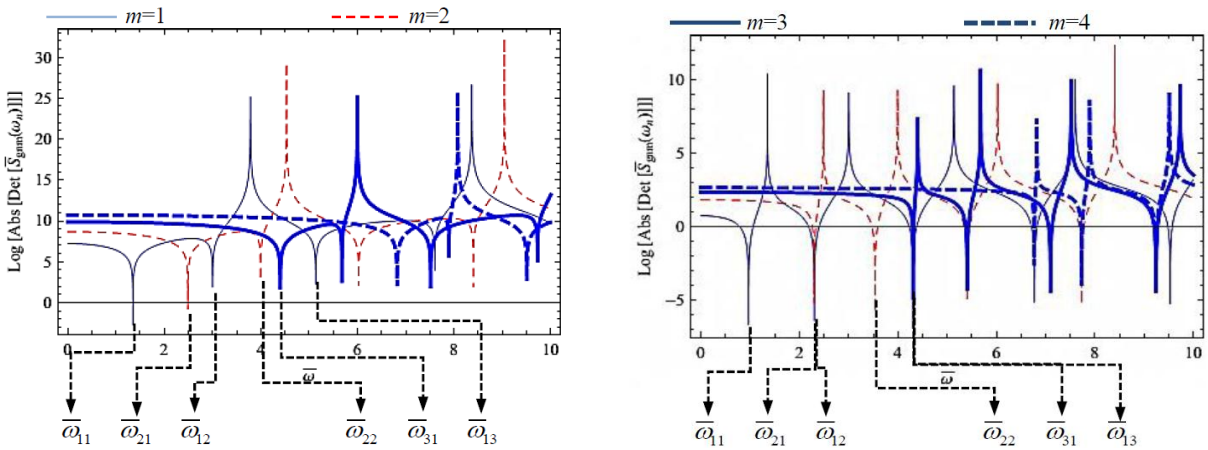

(a) CC (b) SS

Fig.4
Natural frequencies extraction of stationary Levy-type square plate for boundary conditions CC and SS.

In Table 1. the first nine frequency parameters are compared with the results of exact closed form solution and dynamic stiffness method offered by Hosseini-Hashemi et al. [25], and Boscolo and Banerjee [26], respectively, based on FSDT for different boundary conditions (CC, CS and SS). In Table 1 frequency parameters are also compared with the results presented by Liew et al. [27] that obtained from a two dimensional Rayleigh-Ritz method. In this approach, the shear correction factor is 5/6 for free vibration analysis of the moderately thick plates.

Maximum of two finite elements in x-direction are used to obtain the results of spectral finite element formulation. As it could be observed, proposed SFEM with a minimum number of finite elements produces exact results, compared with other exact analytical methods available and numerical methods. The dimensionless frequency parameter obtained from the SFEM and exact analytical methods are in excellent agreement. Therefore, this procedure could effectively be used for the purpose of modeling plate structures with more than one finite element (for example, multi-span plates, stepped thickness plates and plates with internal support).

The dynamic stability of moving Levy-type rectangular plate subjected to uniform in-plane loads for different boundary conditions (CC, CS and SS) was studied. Table 2. shows the dimensionless critical speed ψ_{cr} of the moving Levy-type rectangular plate with different aspect ratios L_y/L_x and different uniform in-plane load parameter k_x, obtained by the spectral finite element method based on FSDT. For confidence, these results are compared with the results reported in Ref. [12] according to CPT. Also, dimensionless fundamental frequencies $\bar{\omega}_1$ of these plates for boundary conditions CC and SS is presented in Table 3. The dimensionless fundamental frequencies of Levy-type rectangular plate subjected to uniform in-plane loads for two cases (stationary and moving situations) are investigated. The axially speed of the moving plate is considered half of their critical speeds which are listed in Table 2. The results are compared with those obtained in Ref [12] based on the classical plate theory.

Table 1
Comparison of the dimensionless natural frequencies $\bar{\omega}$ a Levy-type square plate when L_x/h=10, v=0.3, k =5/6, N_{xx}=0, c=0.

B.C.	Method	Mode sequences								
		1	2	3	4	5	6	7	8	9
CC	Present SFEM	1.35103	2.48809	2.99962	3.99271	4.39957	5.13557	5.67694	6.02466	6.81867
	(m,n)	(1,1)	(2,1)	(1,2)	(2,2)	(3,1)	(1,3)	(3,2)	(2,3)	(4,1)
	CFS [25]	1.35103	2.48809	2.99962	3.99271	4.39957	5.13555	5.67694	6.02466	6.81867
	DSM [26]	1.35103	2.48809	2.99962	3.99271	4.39957	5.13551	5.67692	6.02466	6.81866
	Rayleigh-Ritz Method [27]	1.35105	2.4881	2.9996	3.9927	4.39955	5.13555	5.6770	6.02465	6.81875
CS	Present SFEM	1.13422	2.38631	2.64193	3.75421	4.35052	4.72292	5.53516	5.71153	6.79281
	(m,n)	(1,1)	(2,1)	(1,2)	(2,2)	(3,1)	(1,3)	(3,2)	(2,3)	(4,1)
	CFS [25]	1.13422	2.38631	2.64193	3.75421	4.35052	4.72292	5.53515	5.71153	6.79281
	DSM [26]	1.13422	2.38631	2.64193	3.75421	4.35052	4.72292	5.53513	5.71153	6.79277
	Rayleigh-Ritz Method [27]	1.1342	2.3863	2.64195	3.7542	4.35055	4.72295	5.53515	5.71155	6.79285
SS	Present SFEM	0.96584	2.30418	2.30418	3.53583	4.30808	4.30808	5.40465	5.40465	6.76933
	(m,n)	(1,1)	(1,2)	(2,1)	(2,2)	(1,3)	(3,1)	(2,3)	(3,2)	(1,4)
	CFS [25]	0.96584	2.30418	2.30418	3.53582	4.30808	4.30808	5.40465	5.40465	6.76933
	DSM [26]	0.96584	2.30418	2.30418	3.53583	4.30808	4.30808	5.40462	5.40462	6.76932
	Rayleigh-Ritz Method [27]	0.96585	2.3042	2.3042	3.5358	4.3081	4.3081	5.40465	5.40465	6.76935

Table 2
Comparison of the dimensionless critical speed ψ_{cr} a traveling Levy-type rectangular plate subjected to uniform in-plane loads when L_x/h=500, v=0.3, k =5/6.

B.C.	L_y/L_x	k_x=0		k_x=4	
		Present SFEM, FSDT	EFSM, CPT [12]	Present SFEM, FSDT	EFSM, CPT [12]
CC	10/3	6.8198	6.8200	7.1070	7.1072
	1	2.5967	2.5968	3.2776	3.2777
	3/10	2.0737	2.0741	2.8809	2.8813
CS	10/3	4.9803	4.9803	5.3668	5.3669
	1	2.2016	2.2016	2.9744	2.9744
	3/10	2.0206	2.0209	2.8430	2.8432
SS	10/3	3.6333	3.6333	4.1474	4.1474
	1	2.0000	2.0000	2.8284	2.8284
	3/10	2.0108	2.0111	2.83604	2.8363

Table 3
Comparison of the dimensionless fundamental frequencies $\bar{\omega}_1$ a stationary and moving rectangular plate subjected to uniform in-plane loads when L_x/h=500, v=0.3, k =5/6.

B.C.	L_y/L_x	ψ/ψ_{cr}	k_x=0		k_x=4	
			Present SFEM, FSDT	EFSM, CPT [12]	Present SFEM, FSDT	EFSM, CPT [12]
CC	10/3	0.0	12.8748	12.87525	13.3997	13.40013
		0.5	10.4133	10.41370	10.8054	10.80576
	1	0.0	1.4666	1.46667	1.8309	1.83092
		0.5	1.1588	1.15886	1.4266	1.42661
	3/10	0.0	0.55924	0.55929	0.64119	0.64125
		0.5	0.42002	0.42005	0.49836	0.49839
SS	10/3	0.0	6.0555	6.05556	6.9123	6.91237
		0.5	5.0962	5.09621	5.7796	5.77970
	1	0.0	1.0000	1.00000	1.4142	1.41421
		0.5	0.8038	0.80387	1.1114	1.11137
	3/10	0.0	0.54495	0.54500	0.62207	0.62211
		0.5	0.41389	0.41393	0.48642	0.48723

5.2 Examples

In Sec. 5.1, by the comparison of the natural frequencies of stationary plate obtained using the present method and the CFS, the accuracy of the dynamic stiffness matrix can be ensured. As well as, by the comparison of the natural frequencies and critical speed of moving plate obtained using the present method and EFSM, we can ensure the accuracy of the spectral finite element formulation to obtain the dynamic responses. As a result, the present method can be used to obtain the dynamic responses of the axially moving moderately thick rectangular plates. In this section several examples are represented to show the ability of the proposed SFEM for solving various problems of traveling FSDT plates.

Consider an axially moving moderately thick square plate of Levy-type with boundary condition CC. The geometric and mechanical properties of the plate are L_x/h=5, v=0.3, k =5/6. In this example, four values of 0, 2, 4 and 6 for the non-dimensional uniform in-plane tension are selected. The non-dimensional fundamental frequency $\bar{\omega}_1$ is present as a function of the non-dimensional axial speed ψ and the uniform in-plane load parameter k_x in Fig. 5. The two spectral finite elements in x-direction are used to obtain the exact results by the proposed spectral finite element formulation. As shown in the Fig. 5, the natural frequency decreases with increasing axial moving speed till the speed reach its critical value. The natural fundamental frequency in a constant speed, increases with increasing in-plane tension. In addition, Fig. 5 also indicates that when the uniform in-plane tension increases, the critical speed increases as well.

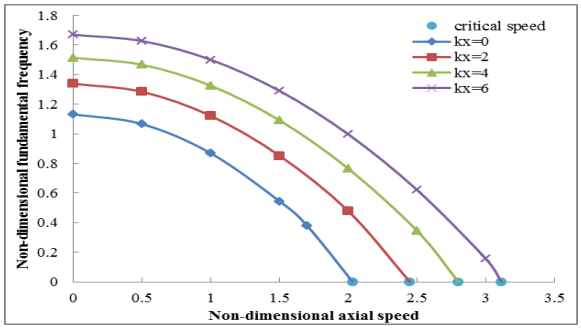

Fig.5
The effect of transport speed on the fundamental frequency of a moderately thick square plate subjected to uniform in-plane load with boundary condition CC (L_x/h=5, v=0.3, k =5/6).

The first five dimensionless natural frequencies of the Levy-type square plate with boundary condition SS for stationary and moving situations are shown in Table 4. The one spectral finite elements in x-direction are used to obtain the exact results. For assurance of the accuracy of the results, the exact results for the stationary plate (c=0) is compared with the results reported in Ref. [25]. As shown in the Table 4. ,the natural frequency increases when in-plane tension increases.

In another example, an isotropic rectangular plate with length to thickness ratio of 5 (L_x/h=5) is considered and the shear correction factor and Poisson's ratio are assumed as 5/6 and 0.3, respectively. The results are extracted for three types of boundary conditions as CC, CS and SS. The dimensionless axial speed ψ and the dimensionless uniform in-plane tension k_x are considered in the calculation as constant values 1 and 15, respectively. The variation of the dimensionless fundamental frequencies $\bar{\omega}_1$ against aspect ratio L_x/L_y for an axially moving plate subjected uniform in-plane tension is given in Fig. 6. The larger aspect ratio leads to the smaller the natural frequencies for a fixed axial speed and the uniform in-plane tension.

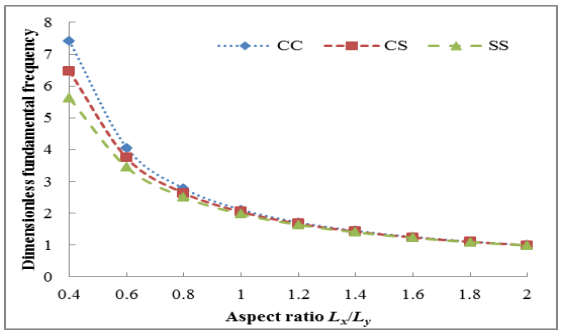

Fig.6
Variation of the dimensionless fundamental frequency against the aspect ratio for a moving rectangular plate subjected to uniform in-plane load (L_x/h=5, v=0.3, k =5/6, k_x=15, ψ=1).

Table 4
The effects of length to thickness ratio (L_x/h) on the dimensionless natural frequencies $\bar{\omega}_1$ a Levy-type square plate with boundary condition SS and when v=0.3, k =5/6.

Dimensionless axial speed ψ	Dimensionless axial tension k_x	L_x/h	Method	Dimensionless natural frequency				
				$\bar{\omega}_1$	$\bar{\omega}_2$	$\bar{\omega}_3$	$\bar{\omega}_4$	$\bar{\omega}_5$
0	0	10	Present SFEM	0.9658	2.3042	2.3042	3.5358	4.3081
			CFS [25]	0.9658	2.3042	2.3042	3.5358	4.3081
		5	Present SFEM	0.8839	1.9328	1.9328	2.7939	3.3003
			CFS [25]	0.8839	1.9328	1.9328	2.7939	3.3003
0	4	15		1.4007	2.6023	3.1183	4.2548	4.7500
		10	Present SFEM	1.3850	2.5057	3.0307	4.0411	4.4171
		5		1.3184	2.1605	2.7307	3.3901	3.4370
0.5 ψ_{cr} *	4	15		1.0952	2.3420	2.7258	3.8970	4.4865
		10	Present SFEM	1.0770	2.2326	2.6055	3.6410	4.1268
		5		1.0040	1.8520	2.2097	2.8728	3.0787

* L_x =15h: ψ_{cr}=2.8014, L_x =10h: ψ_{cr}=2.7700, L_x =5h: ψ_{cr}=2.6368

To draw mode shapes of the moderately thick plate, use is made of dynamic shape function (N^T_{Wnm} , $N^T_{\Phi xnm}$ and $N^T_{\Phi ynm}$) corresponding to spectral-modal displacements (W_{nm}, Φ_{xnm} and Φ_{ynm}), as presented in Sec. 3.2.3. The mode shapes for the first mode (m=1, n=1) and the second mode (m=2, n=1) are plotted. In Fig. 7, mode shapes of the square plate for boundary condition CC are shown. Figs. 7(a)-7(c) show mode shapes for the transverse displacement of the stationary plate (k_x=0, ψ=0), the stationary plate subjected uniform in-plane loads (k_x=10, ψ=0) and the axially moving plate (k_x=10, ψ=2), respectively. It should be noted that according to Eqs. (20), variation of W_{nm} and Φ_{xnm} along the y axis is in sine form and variation of Φ_{ynm} is in cosine form. As shown in Figs. 7(c) the mode shapes for the moving plate are the complex values.

The Levy-type rectangular plate with width L_y and thickness h equal to 1 and 0.1 m, respectively, are considered and the shear correction factor and Poisson's ratio are assumed as 5/6 and 0.3, respectively. The uniform in-plane tension parameter k_x are considered in the calculation as constant value 15. Table 5. shows the dimensionless critical speed ψ_{cr} of the axially moving Levy-type rectangular plate subjected uniform in-plane tension with different aspect ratios L_x/L_y and boundary conditions (CC, CS and SS), obtained by the spectral finite element method based on FSDT. The larger aspect ratio (L_x/L_y) leads to the smaller the critical speed for a fixed the uniform in-plane tension. It can also be seen that the plates with boundary conditions CC and SS have the highest and lowest critical speed, respectively.

Table 5
The first dimensionless critical speed ψ_{cr} a traveling Levy-type rectangular plate subjected to uniform in-plane loads when L_y=1 m, h=0.1 m, v=0.3, k =5/6, k_x=15.

B.C.	Aspect ratio (L_x/L_y)									
	0.1	0.2	0.3	0.4	0.5	1	1.5	2	2.5	3
CC	6.52341	6.22272	5.71755	5.33551	5.06004	4.50560	4.42417	4.36577	4.34808	4.33199
CS	6.45361	5.74579	5.23909	4.91102	4.70182	4.36577	4.34408	4.31901	4.31564	4.30926
SS	6.21931	5.32636	4.84556	4.59270	4.45429	4.30261	4.31924	4.30261	4.30589	4.30261

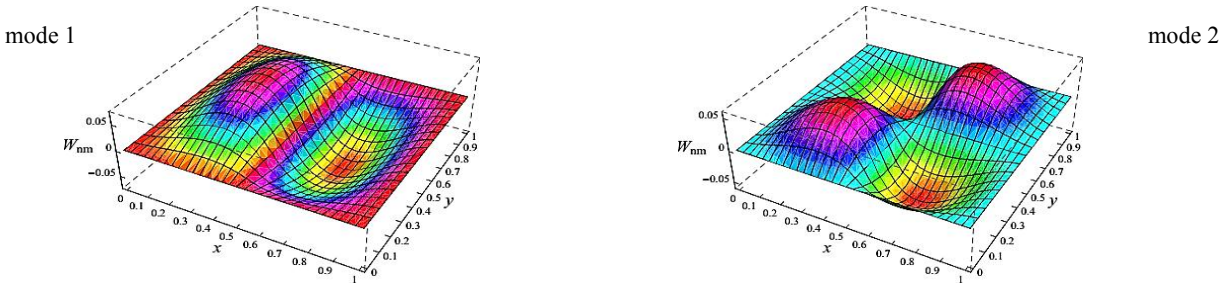

(a) stationary plate; k_x=0, ψ=0

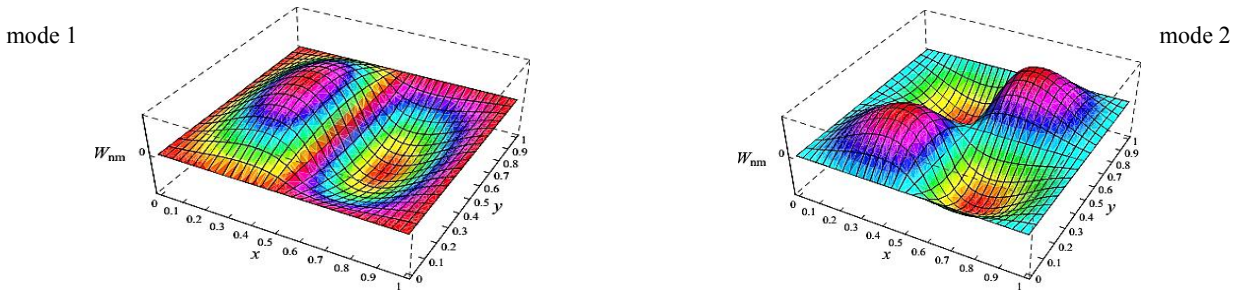

(b) stationary plate subjected uniform in-plane loads; k_x=10, ψ=0

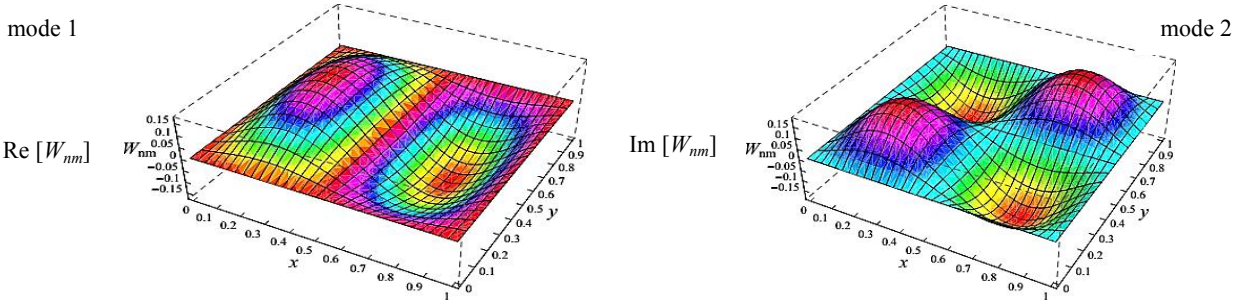

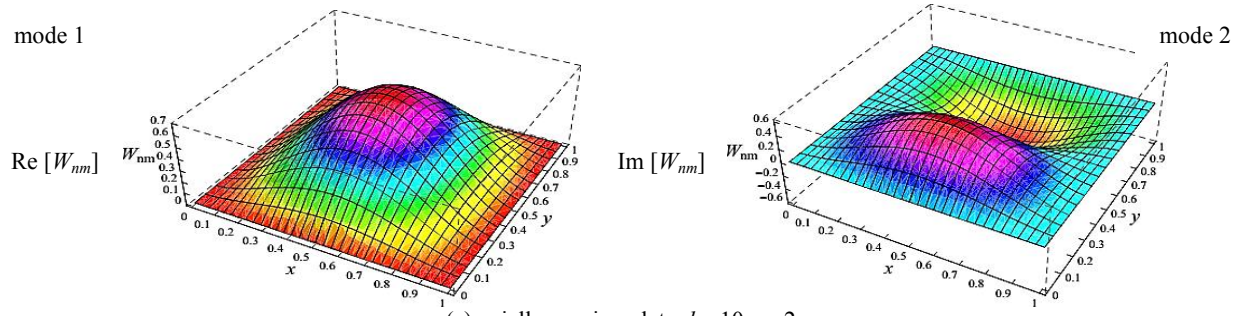

(c) axially moving plate; k_x=10, ψ=2

Fig.7
First two mode shapes of the stationary and moving Levy-type square plate with boundary conditions CC (L_x/h=10, h=0.1 m, ν=0.3, k =5/6).

6 CONCLUSIONS

The transverse free vibration of the Levy-type moderately thick rectangular plates axially moving with constant velocity and subjected to uniform in-plane loads was studied by the spectral finite element method based on first-order shear deformation theory. The spectral stiffness matrix obtained in the present SFEM is a transcendental function of natural frequencies, axial speed, in-plane loads and half-wavelengths. Since the frequency-dependent dynamic shape functions in SFEM are obtained from the exact solution of the governing differential equations of motion of the plate, increasing the number of spectral element to achieve the exact answers is not required. The results obtained by the spectral finite element formulation need maximum of two finite elements in x-direction. As is noticeable, the proposed SFEM achieves exact results with minimal finite elements, compared with exact analytical methods and numerical methods. Therefore, it is possible to effectively use this procedure for the plate structures and other plates in which more than one finite element is needed for modeling purposes.

The exactness and validity of the results is verified by comparing them with the results in the other studies. By the developed method some examples for vibration of stationary and moving moderately thick plates with different boundary conditions are presented. The effects of some parameters such as the axially speed of plate motion, the in-plane forces, aspect ratio and length to thickness ratio on the natural frequencies and the critical speeds of the moving plate are investigated.

REFERENCES

[1] Ulsoy A.G., Mote C.D.Jr., 1982, Vibration of wide band saw blades, *Journal of Engineering for Industry* **104**: 71-78.

[2] Lengoc L., McCallion H., 1995, Wide bandsaw blade under cutting conditions, part I: vibration of a plate moving in its plane while subjected to tangential edge loading, *Journal of Sound and Vibration* **186**(1): 125-142.

[3] Wang X., 1999, Numerical analysis of moving orthotropic thin plates, *Computers and Structures* **70**: 467-486.

[4] Luo Z., Hutton S.G., 2002, Formulation of a three-node traveling triangular plate element subjected to gyroscopic and inplane forces, *Computers and Structures* **80**: 1935-1944.

[5] Zhou Y.F., Wang Z.M., 2008, Vibration of axially moving viscoelastic plate with parabolically varying thickness, *Journal of Sound and Vibration* **316**: 198-210.

[6] Tang Y.Q., Chen L.Q., 2011, Nonlinear free transverse vibrations of in-plane moving plates: without and with internal resonances, *Journal of Sound and Vibration* **330**: 110-126.

[7] An C., Su J., 2014, Dynamic analysis of axially moving orthotropic plates: Integral transform solution *, Applied Mathematics and Computation* **228**: 489-507.

[8] Eftekhari S.A., Jafari A.A., 2014, High accuracy mixed finite element-differential quadrature method for free vibration of axially moving orthotropic plates loaded by linearly varying in-plane stresses, *Transactions B: Mechanical Engineering* **21**(6): 1933-1954.

[9] Lin C.C., 1997, Stability and vibration characteristics of axially moving plates, *International Journal of Solids and Structures* **34**(24): 3179-3190.

[10] Luo A.C.J., Hamidzadeh H.R., 2004, Equilibrium and buckling stability for axially traveling plates, *Communications in Nonlinear Science and Numerical Simulation* **9**: 343-360.

[11] Marynowski K., 2010, Free vibration analysis of the axially moving Levy-type viscoelastic plate, *European Journal of Mechanics A/Solids* **29**: 879-886.

[12] Hatami S., Azhari M., Saadatpour M.M., 2006, Exact and semi-exact finite strip for vibration and dynamic stability of traveling plates with intermediate supports, *Advances in Structural Engineering* **9**(5): 639-651.

[13] Hatami S., Azhari M., Saadatpour M.M., 2006, Stability and vibration of elastically supported, axially moving orthotropic plates, *Transaction B, Engineering* **30**(B4): 427-446.

[14] Hatami S., Azhari M., Saadatpour M.M., 2007, Free vibration of moving laminated composite plates, *Composite Structures* **80**: 609-620.

[15] Hatami S., Ronagh H.R., Azhari M., 2008, Exact free vibration analysis of axially moving viscoelastic plates, *Computers and Structures* **86**: 1738-1746.

[16] Saksa T., Jeronen J., 2015, Estimates for divergence velocities of axially moving orthotropic thin plates, *Mechanics Based Design of Structures and Machines: An International Journal* **43**(3): 294-313.

[17] Oh H., Lee U., Park D.H., 2004, Dynamic of an axially moving Bernouli-Euler beam: spectral element modeling and analysis, *KSME International Journal* **18**(3): 395-406.

[18] Lee U., Kim J., Oh H., 2004, Spectral analysis for the transverse vibration of an axially moving Timoshenko beam, *Journal of Sound and Vibration* **271**: 685-703.

[19] Lee U., Oh H., 2005, Dynamics of an axially moving viscoelastic beam subject to axial tension, *International Journal of Solids and Structures* **42**: 2381-2398.

[20] Kim J., Cho J., Lee U., Park S., 2003, Modal spectral element formulation for axially moving plates subjected to in-plane axial tension, *Computers and Structures* **81**: 2011-2020.

[21] Kwon K., Lee U., 2006, Spectral element modeling and analysis of an axially moving thermoelastic beam-plate, *Journal of Mechanics of Materials and Structures* **1**(1): 605-632.

[22] Reddy J.N., 2007, *Theory and Analysis of Elastic Plates and Shells*, CRC Press, Boca Raton.

[23] Reissner E., 1994, On the theory of bending of elastic plates, *Journal Math Physics* **23**(4): 184-191.

[24] Lee U., 2009, *Spectral Element Method in Structural Dynamics*, John Wiley & Sons, Inc.

[25] Hosseini Hashemi Sh., Arsanjani M., 2005, Exact characteristic equations for some of classical boundary conditions of vibrating moderately thick rectangular plates, *International Journal of Solids and Structures* **42**: 819-853.

[26] Boscolo M., Banerjee J.R., 2011, Dynamic stiffness elements and their applications for plates using first order shear deformation theory, *Computers and Structures* **89**: 395-410.

[27] Liew K.M., Xiang Y., Kitipornchai S., 1993, Transverse vibration of thick rectangular plates-I comprehensive sets of boundary conditions, *Computers and Structures* **49**(1): 1-29.